AMERICAN SOCIETY FOR MICROBIOLOGY | Infection and Immunity®

BACTERIAL INFECTIONS

Role of Sca2 and RickA in the Dissemination of *Rickettsia parkeri* in *Amblyomma maculatum*

Emma K. Harris,[a]* Krit Jirakanwisal,[a] Victoria I. Verhoeve,[a]* Chanida Fongsaran,[a] Chanakan Suwanbongkot,[a] Matthew D. Welch,[b] Kevin R. Macaluso[a]

[a]Vector-Borne Disease Laboratories, Department of Pathobiological Sciences, School of Veterinary Medicine, Louisiana State University, Baton Rouge, Louisiana, USA

[b]Department of Molecular and Cell Biology, University of California, Berkeley, Berkeley, California, USA

ABSTRACT The Gram-negative obligate intracellular bacterium *Rickettsia parkeri* is an emerging tick-borne human pathogen. Recently, *R. parkeri* Sca2 and RickA have been implicated in adherence and actin-based motility in vertebrate host cell infection models; however, the rickettsia-derived factors essential to tick infection are unknown. Using *R. parkeri* mutants lacking functional Sca2 or RickA to compare actin polymerization, replication, and cell-to-cell spread *in vitro*, similar phenotypes in tick and mammalian cells were observed. Specifically, actin polymerization in cultured tick cells is controlled by the two separate proteins in a time-dependent manner. To assess the role of Sca2 and RickA in dissemination in the tick host, *Rickettsia*-free *Amblyomma maculatum*, the natural vector of *R. parkeri*, was exposed to wild-type, *R. parkeri rickA*::*tn*, or *R. parkeri sca2*::*tn* bacteria, and individual tick tissues, including salivary glands, midguts, ovaries, and hemolymph, were analyzed at 12 h and after continued bloodmeal acquisition for 3 or 7 days postexposure. Initially, ticks exposed to wild-type *R. parkeri* had the highest rickettsial load across all organs; however, rickettsial loads decreased and wild-type rickettsiae were cleared from the ovaries at 7 days postexposure. In contrast, ticks exposed to *R. parkeri rickA*::*tn* or *R. parkeri sca2*::*tn* had comparatively lower rickettsial loads, but bacteria persisted in all organs for 7 days. These data suggest that while RickA and Sca2 function in actin polymerization in tick cells, the absence of these proteins did not change dissemination patterns within the tick vector.

KEYWORDS actin-based motility, *Amblyomma maculatum*, RickA, *Rickettsia parkeri*, Sca2

Members of the spotted fever group (SFG) *Rickettsia* are obligate intracellular bacteria transmitted by ticks vertically (between life cycle stages) and horizontally (between ticks) via a vertebrate host. In horizontal acquisition, ticks imbibe an infectious bloodmeal from the vertebrate host, allowing the rickettsiae to enter the gut and then, through undefined mechanisms, disseminate throughout the tick to infect organs central to transmission, including the ovaries (vertical) and salivary glands (horizontal). The ability of individual *Rickettsia* species to successfully infect and be transmitted by a tick host varies by both *Rickettsia* and tick species (1). Transmission of SFG *Rickettsia* to a vertebrate host during tick feeding can result in disease ranging from a mild, self-limiting infection to death (2, 3). The incidence of tick-borne SFG rickettsiosis is on the rise due to increased recognition among physicians, increased geographic distribution of tick vectors, and the emergence of rickettsial pathogens (2, 4, 5). Among the more recently recognized pathogens is *Rickettsia parkeri*, with at least 35 confirmed human cases, not including patients likely misdiagnosed with classic Rocky Mountain spotted fever (6). The molecular factors contributing to rickettsial colonization, maintenance, and transmission within tick vectors have not been identified.

Received 12 February 2018 **Returned for modification** 4 March 2018 **Accepted** 21 March 2018

Accepted manuscript posted online 26 March 2018

Citation Harris EK, Jirakanwisal K, Verhoeve VI, Fongsaran C, Suwanbongkot C, Welch MD, Macaluso KR. 2018. Role of Sca2 and RickA in the dissemination of *Rickettsia parkeri* in *Amblyomma maculatum*. Infect Immun 86:e00123-18. https://doi.org/10.1128/IAI.00123-18.

Editor Guy H. Palmer, Washington State University

Address correspondence to Kevin R. Macaluso, kmacal2@lsu.edu.

* Present address: Emma K. Harris, Centers for Disease Control and Prevention, Division of Vector-Borne Diseases, Fort Collins, Colorado, USA; Victoria I. Verhoeve, Department of Biology, West Virginia University, Morgantown, West Virginia, USA.

It has recently been demonstrated that disruption of two key proteins leading to *R. parkeri* actin-based motility (ABM) negatively impacts intracellular bacterial movement and therefore dissemination from cell to cell in *in vitro* models of mammalian infection (7). One of these proteins, RickA, is a nucleation promoting factor that functions by activating the host cell Arp2/3 complex to mediate actin branching and ABM (7, 8). A second protein, surface cell antigen 2 (Sca2), has also been shown to act as a formin-like mediator of ABM and contributes to mammalian cell adhesion (9–11). Utilizing transposon mutagenesis to generate two strains of *R. parkeri*, one lacking expression of full-length Sca2 and the other lacking RickA, the current model of *R. parkeri* actin-based motility suggests that RickA coordinates early-phase motility (15 to 30 min postinfection), giving rise to short actin tails and slow bacterial movement. Alternatively, late-phase motility (24 to 48 h postinfection) is mediated by Sca2, resulting in more elongated actin tails and increased rickettsial velocity within the cell (7). While progress has been made toward understanding the role of rickettsial proteins in vertebrate host cell infection, their function in arthropod cells and during infection and dissemination in the tick vector is unknown.

In this study, the phenotypes of RickA- and Sca2-deficient *R. parkeri* were assessed in an arthropod host cell background *in vitro* to determine if strategies of ABM utilized in the tick host are similar to those reported for vertebrate host cells. Additionally, infection and dissemination dynamics of *R. parkeri* wild-type, *rickA*::*tn*, and *sca2*::*tn* strains in the tick vector *Amblyomma maculatum* were evaluated to determine if ABM orchestrated by rickettsial Sca2 and RickA contributes to *R. parkeri* dissemination within its tick host. Similar phenotypes were observed by comparing vertebrate and tick host cell backgrounds, and while all strains were able to disseminate in the tick after acquisition, the wild-type strain resulted in a greater bacterial load with a diminished ability to persist in tick reproductive tissue.

RESULTS

Actin polymerization of *R. parkeri* in arthropod cells is comparable to that in mammalian cells. To define the temporal pattern of *R. parkeri* motility, ISE6 cells were infected and ABM assessed at several time points. Tandem experiments in Vero cells were completed to act as a positive control for previously established actin polymerization patterns (7). *Rickettsia* was observed to actively polymerize actin at both 30 min postinfection (mpi) and 48 h postinfection (hpi) in Vero and ISE6 cells (Fig. 1A to D). Less than 5% of wild-type *R. parkeri* was observed to polymerize actin after 30 min of infection in ISE6 cells (Fig. 1E). Maximum polymerization was observed at 2 hpi in Vero cells and at 24 hpi in ISE6 cells (Fig. 1E). High-magnification images of ABM in ISE6 cells were visualized at 48 hpi, demonstrating a similarity to that previously shown in mammalian cells (see Fig. S1 in the supplemental material) (7–9, 12, 13). Expression of RickA and Sca2 in wild-type *R. parkeri* in tick cells matched observations in Vero cells with nonsignificant inverse expression of RickA and Sca2 (Fig. 1F to I). Overall, these data show that wild-type *R. parkeri* actin polymerization occurs in both Vero and ISE6 cells.

Rickettsial mutants lacking Sca2 or RickA replicate similarly to wild-type *R. parkeri* in tick cells. To assess potential differences in growth kinetics between wild-type *R. parkeri* and *sca2*::*tn* or *rickA*::*tn* strains in tick-derived cells, rickettsiae were grown in Vero and tick cells for 120 h. Replication of both *R. parkeri sca2*::*tn* and *R. parkeri rickA*::*tn* strains was similar to that of the wild-type *R. parkeri* in Vero and ISE6 cell lines (Fig. 2A and B). Overall replication rates were greater in ISE6 cells than in Vero cells, with rickettsial density increasing approximately 100-fold for all three strains. However, there was no significant difference between the replication of the mutant strains and wild-type *R. parkeri* in either host cell background. Therefore, rickettsial Sca2 and RickA are not required for replication within cells *in vitro*, independent of host cell origin. Additionally, assessment of expression of Sca2 and RickA expression in respective mutant strains was carried out via Western blotting. Results showed that Sca2 expression was not present in *R. parkeri sca2*::*tn* samples but was consistently observed at 75

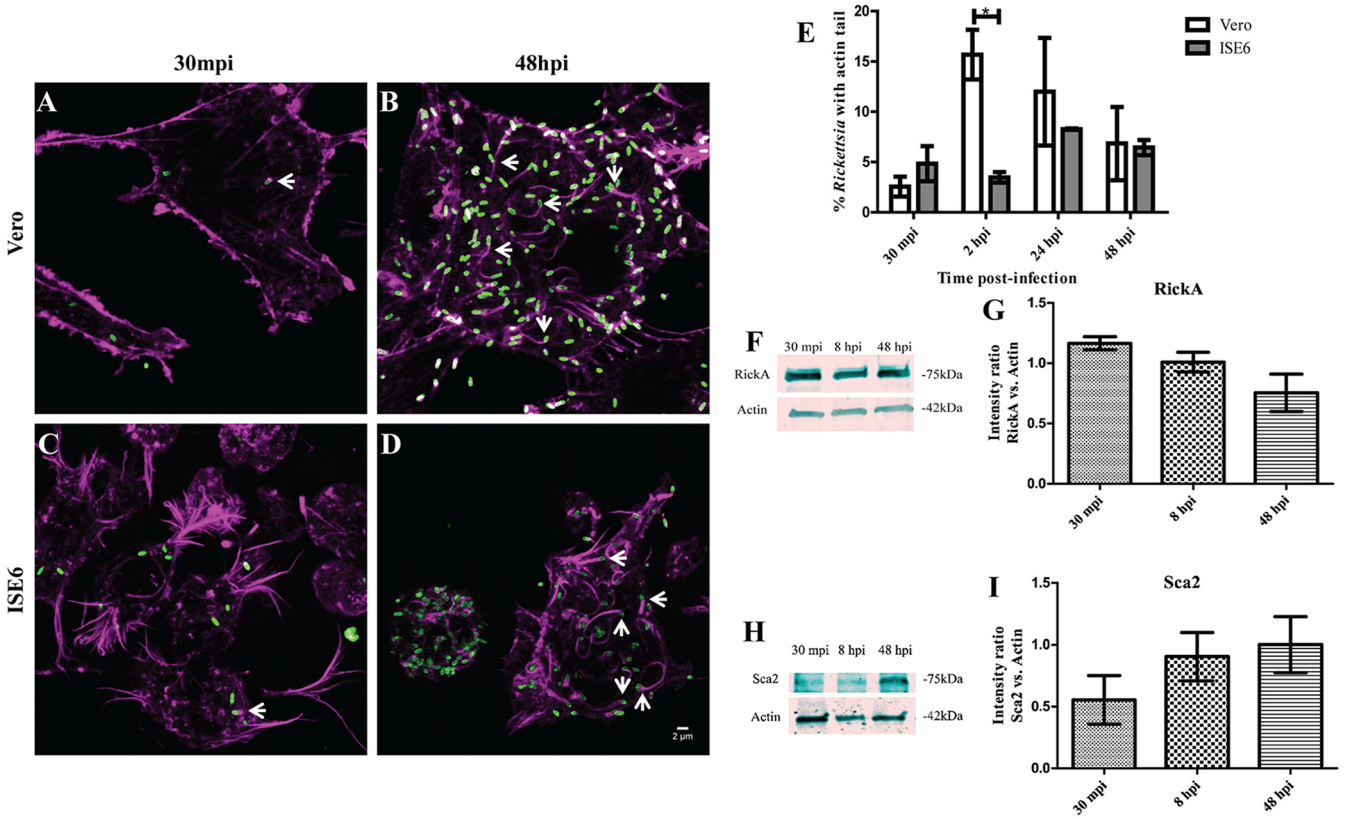

FIG 1 Actin polymerization of *R. parkeri* in Vero and ISE6 cells and expression of Sca2 and RickA in ISE6 cells. (A and B) Wild-type *R. parkeri* (green) polymerizing actin (magenta) in Vero cells at 30 mpi and 48 hpi. (C and D) Wild-type *R. parkeri* (green) polymerizing actin (magenta) in ISE6 cells 30 mpi and 48 hpi. White scale bar, 2 μm. Arrows indicate *Rickettsia* polymerizing actin. (E) Percentage of wild-type *R. parkeri* present in Vero and ISE6 cells with an actin tail at 30 mpi and 2, 24, and 48 hpi. Bacteria with and without actin tails were recorded at each time point postinfection in order to determine the profile of *R. parkeri* actin polymerization. Error bars represent the standard errors of the means. Data are representative of two replicates per experiment and two independent experiments. Ten images taken across all experimental replicates were used in analyses. (F and G) Western blot (F) and corresponding graph (G) of RickA expression normalized against ISE6 expression of β-actin at 30 mpi and 8 and 48 hpi for wild-type *R. parkeri*. (H and I) Western blot (H) and corresponding graph (I) of Sca2 expression normalized against ISE6 expression of β-actin at 30 mpi and 8 and 48 hpi for wild-type *R. parkeri*. Statistical analysis consisted of a one-way ANOVA followed by Tukey's *post hoc* analysis (G and I) or an unpaired *t* test (E), with a *P* value of <0.05 considered significant (denoted by an asterisk). Data are representative of two replicates per experiment and two independent experiments.

kDa in *R. parkeri rickA*::*tn* samples (Fig. 2C). Conversely, RickA expression was detected in *R. parkeri sca2*::*tn* samples and weakly in *R. parkeri rickA*::*tn* samples (Fig. 2D).

Time-dependent ABM occurs in tick cells *in vitro*. Previous analyses in mammalian cells suggest that early-phase (30 mpi) ABM is driven by RickA and late-phase ABM (24 to 48 hpi) is initiated by Sca2 (7). Wild-type *R. parkeri* demonstrated actin polymerization at 30 mpi in both cell types (Fig. 3A and E). Utilizing fluorescence microscopy to visualize infected cells, it was determined that *R. parkeri sca2*::*tn* also employs actin polymerization at 30 mpi in both Vero and ISE6 cells (Fig. 3B and F). However, for *R. parkeri rickA*::*tn*, ABM was not observed at 30 mpi (Fig. 3C and G), demonstrating that similar to mammalian *in vitro* infection, early-phase rickettsial motility in arthropod cells is coordinated by RickA. The percentage of total rickettsiae polymerizing actin in either cell type did not differ between wild-type and mutant *R. parkeri* at 30 mpi (Fig. 3D and H). At 48 hpi, actin polymerization was observed in Vero and ISE6 cells for both wild-type *R. parkeri* and *rickA*::*tn* strains (Fig. 4A, C, E, and F), while the *sca2*::*tn* strain did not polymerize actin (Fig. 4B and F). In addition to no actin polymerization by *R. parkeri sca2*::*tn*, there was a significant decrease in ABM observed in the *rickA*::*tn* strain compared to that of wild-type *R. parkeri* in tick cells only (Fig. 4D and H). Similar to the phenotype observed in Vero cells, actin polymerization in tick cells is controlled by two separate proteins in a time-dependent manner.

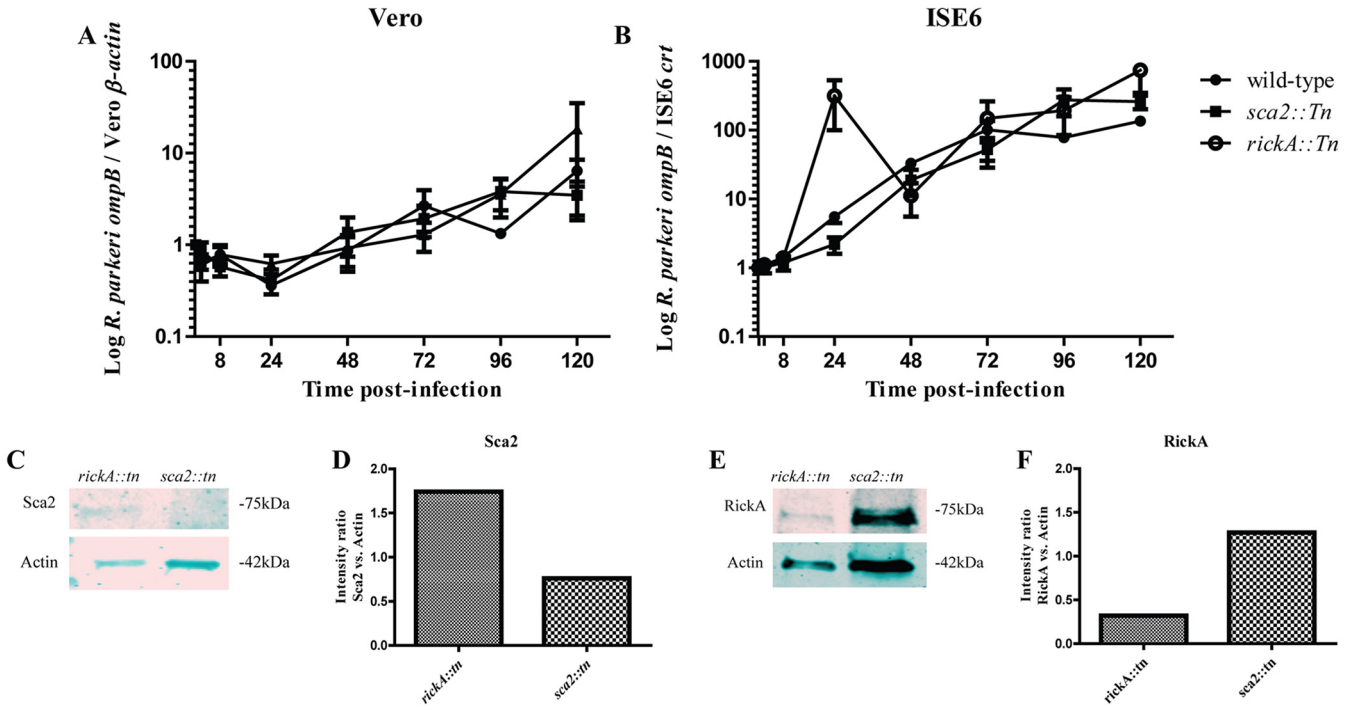

FIG 2 Growth curves for *R. parkeri* wild-type, *sca2*::*tn*, and *rickA*::*tn* strains in Vero (A) and ISE6 (B) cells. Data are fold change compared to initial input. Collection times consisted of 30 mpi and 2, 8, 24, 48, 72, 96, and 120 hpi. There was a lack of statistical significance at all time points for *R. parkeri sca2*::*tn* and *rickA*::*tn* strains compared to wild-type *R. parkeri* across both cell types. Data are representative of three replicates per experiment and two independent experiments. A Kruskal-Wallis test with Dunn's *post hoc* analysis was completed in GraphPad Prism software. A *P* value of <0.05 was considered significant. Western blots showing expression or lack of expression of Sca2 (C) and RickA (E) in *R. parkeri sca2*::*tn* and *rickA*::*tn*. Densitometric analysis of Sca2 (D) and RickA (F) expression in respective mutant strains was completed by normalizing expression of each protein against expression of β-actin in Vero cells.

Cell-to-cell spread of *R. parkeri rickA*::*tn* is significantly reduced in tick cells. A cell-to-cell spread assay was employed to determine the effect that loss of RickA or Sca2 had on dissemination of *R. parkeri* in cultured cells. A significant decrease in rickettsial spread to neighboring cells was observed for both *R. parkeri rickA*::*tn* and *sca2*::*tn* in Vero cells (Fig. 5A to D). In ISE6 cells, a significant decrease in rickettsial dissemination was observed only for *R. parkeri rickA*::*tn* (Fig. 5E to H). This demonstrates that rickettsial infection in mammalian, but not arthropod, cells is impacted by the disruption of both *rickA* and *sca2*.

Dissemination of *R. parkeri* in *A. maculatum* does not depend on Sca2 or RickA. The role of RickA and Sca2 was investigated *in vivo* by infecting *A. maculatum* ticks via a previously published capillary feeding technique to expose ticks to a dose of 5×10^7 rickettsiae/μl (1, 14). At 12 h postexposure (hpe), among the treatment groups, rickettsiae were detected in 75 to 100% of exposed ticks, demonstrating effective acquisition of rickettsiae. There was no significant difference in rickettsial density between organs within each strain (i.e., levels of wild-type *R. parkeri* in the midgut versus that in the salivary glands). In the midgut, no significant difference between wild-type *R. parkeri* load and *R. parkeri sca2*::*tn* or *rickA*::*tn* was detected. In the ovaries, wild-type *R. parkeri* had a significantly higher rickettsial burden than either of the mutant strains (Fig. 6A, C, and E). Microscopic evaluation of each organ (Fig. S2) for the presence of rickettsiae and actin tail formation was conducted; however, while all three strains of *Rickettsia* were detected, no evidence of ABM was observed (Fig. 6B, D, and F and Fig. S3). These data demonstrate that rickettsial dissemination into all major organs occurs after 12 h of capillary feeding. Additionally, rickettsial mutants are not deficient in infecting the midgut or salivary glands compared to the wild-type parent strain. However, infection in the ovaries was significantly lower at 12 h than that of the wild-type strain. While differences in bacterial density were observed, the lack of a

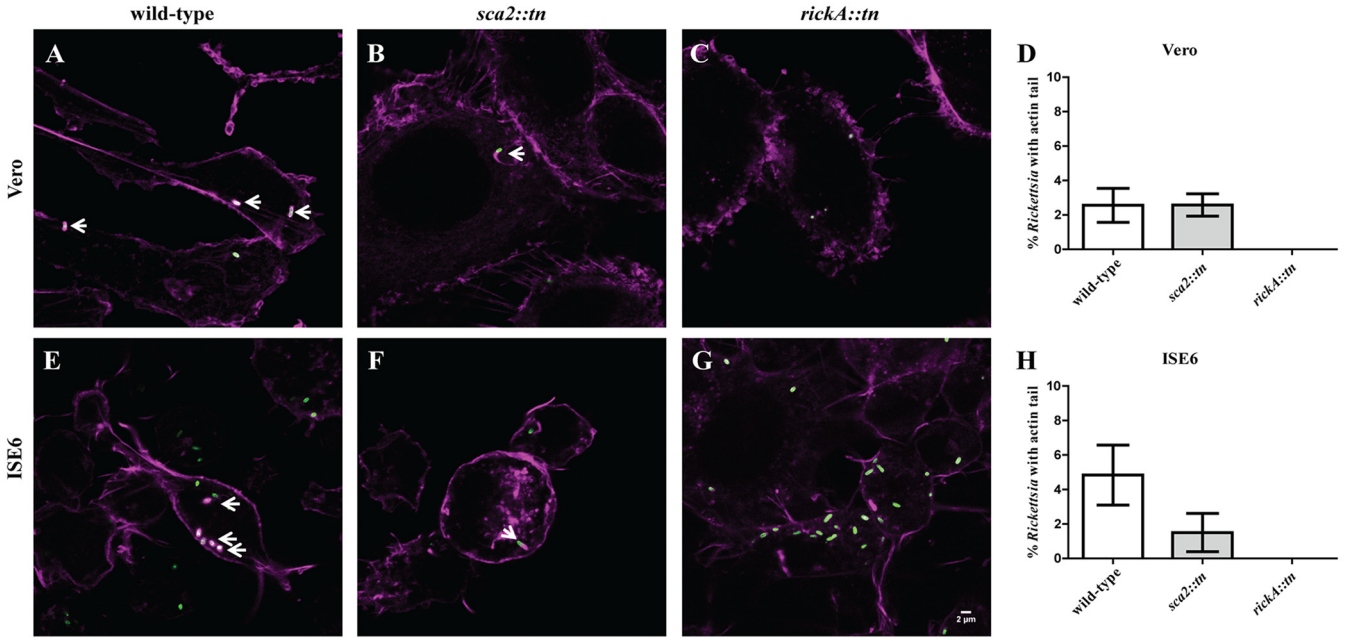

FIG 3 Actin polymerization profile of wild-type *R. parkeri* compared to *R. parkeri sca2*::*tn* and *rickA*::*tn* in Vero and ISE6 cells at 30 mpi. *Rickettsia* (green) actively polymerizing actin (magenta) in Vero (A to C) and ISE6 (E to G) cells is shown. This assay was repeated for *R. parkeri* wild-type (A and E), *R. parkeri sca2*::*tn* (B and F), and *R. parkeri rickA*::*tn* (C and G) strains. (D and H) Graphical representation of percent *Rickettsia* with an actin tail in Vero (D) and ISE6 (H) cells. Data are representative of two replicates per experiment and two independent experiments. Statistical analysis consisted of a *t* test. $P < 0.05$. White scale bar, 2 μm. Arrows indicate *Rickettsia* polymerizing actin.

distinct dissemination phenotype suggests that neither Sca2 nor RickA alone is essential for early infection in the tick host.

Following the establishment of a dissemination profile at 12 hpe, an assessment of the contributing role of Sca2 and RickA in bacterial persistence within the feeding tick was investigated. After 3 days of additional bloodmeal acquisition, ticks ($n = 3$ to 8 ticks/strain) were forcibly removed from the host and rickettsial infection was assessed. For this group, 50 to 100% of the individual organs exposed to either wild-type *R. parkeri* or mutant strains were infected. Compared to results at 12 hpe, rickettsial density in each organ was 1 to 2 logs lower at 3 days postexposure (dpe). Midguts, salivary glands, and ovaries had variable densities of all strains of *R. parkeri*, with no significant differences between each organ or rickettsial strain (Fig. 7A, C, and E). These data demonstrate that disseminated *R. parkeri* infection is sustained 3 dpe in a feeding tick, which was also confirmed via microscopy (Fig. 7B, D, and F). Numbers of *R. parkeri rickA*::*tn*-infected ticks were lower at 3 dpe due to death postexposure; however, no distinct phenotype was observed for rickettsial mutants compared to wild-type *R. parkeri*, further indicating dissemination in the vector occurs independently of RickA or Sca2.

Female *A. maculatum* can feed for an extended period of time (~10 days); therefore, to further investigate the dissemination and persistence pattern of wild-type *R. parkeri* compared to *R. parkeri sca2*::*tn* and *rickA*::*tn*, ticks ($n = 6$ to 7 ticks/strain) were allowed to feed on host for 7 dpe. Infection of *A. maculatum* organs at 7 dpe ranged from 0 to 67% of exposed tick tissues. Rickettsial strains were 1 to 2 logs lower at 7 dpe than at 3 dpe for each organ. All strains of *R. parkeri* were detected by qPCR in the midgut and salivary glands for 7 dpe (Fig. 8A and C), demonstrating a persistent infection phenotype in these organs independent of infecting strain. In tick ovaries, *R. parkeri sca2*::*tn* and *rickA*::*tn*, but not wild type, were detected by qPCR (Fig. 8E). Rickettsiae were identified by microscopy in all tissues (Fig. 8B, D, and F), even in the absence of qPCR-positive samples for wild-type *R. parkeri*; however, staining was not appreciable when compared to no-primary-antibody control images for each set of organs, which identified limited, nonspecific binding (Fig. S4). Statistical inferences could not be made

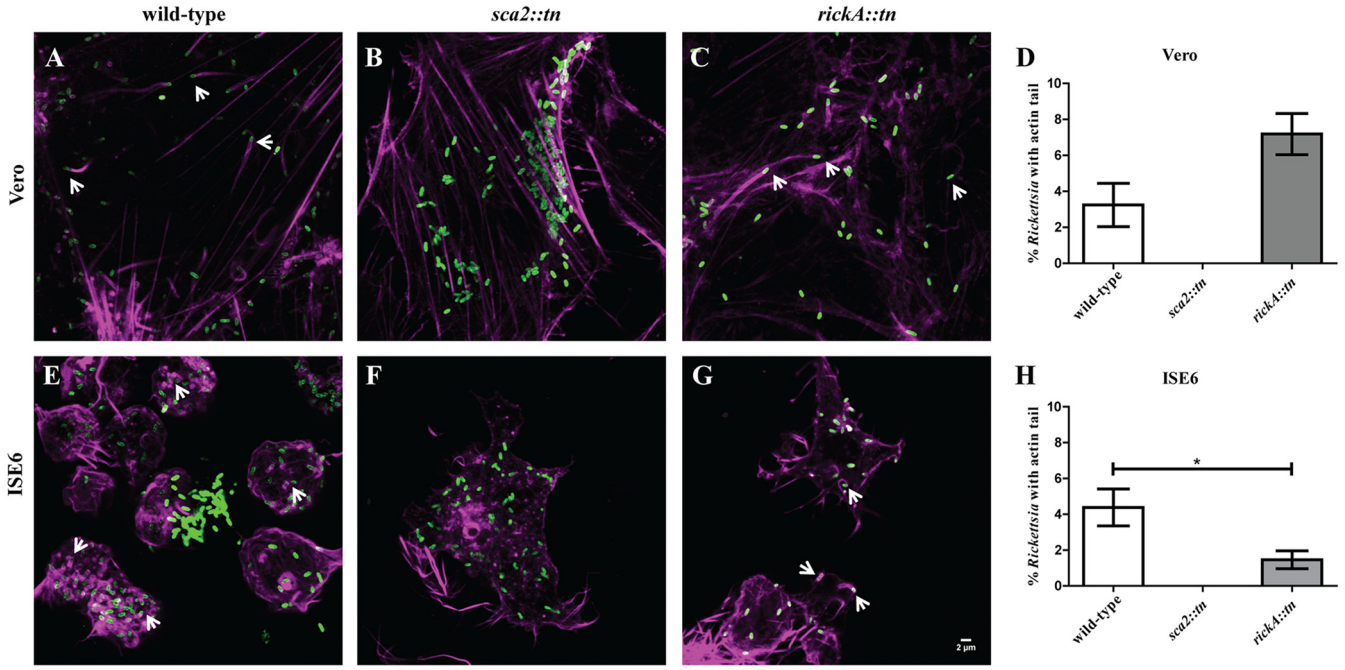

FIG 4 Actin polymerization of wild-type *R. parkeri* compared to that of *R. parkeri sca2*::*tn* and *rickA*::*tn* in Vero and ISE6 cells at 48 hpi. *Rickettsia* (green) actively polymerizing actin (magenta) in Vero (A to C) and ISE6 (E to G) cells is shown. Wild-type *R. parkeri* (A and E), *R. parkeri sca2*::*tn* (B and F), and *R. parkeri rickA*::*tn* (C and G) strains are depicted. (D and H) Graphical representation of percent *Rickettsia* with actin tails in Vero (D) and ISE6 (H) cells. Data are representative of two replicates per experiment and two independent experiments. Statistical analysis consisted of a *t* test, with a *P* value of <0.05 being significant. White scale bar, 2 μm. Arrows indicate *Rickettsia* polymerizing actin.

comparing the wild-type *R. parkeri* and the *R. parkeri sca2*::*tn* and *R. parkeri rickA*::*tn* strains due to low numbers of infected ticks at 7 dpe. Although the mean rickettsial load decreased during tick feeding postexposure, *R. parkeri* organisms lacking expression of Sca2 and RickA were still able to infect and persist in *A. maculatum*.

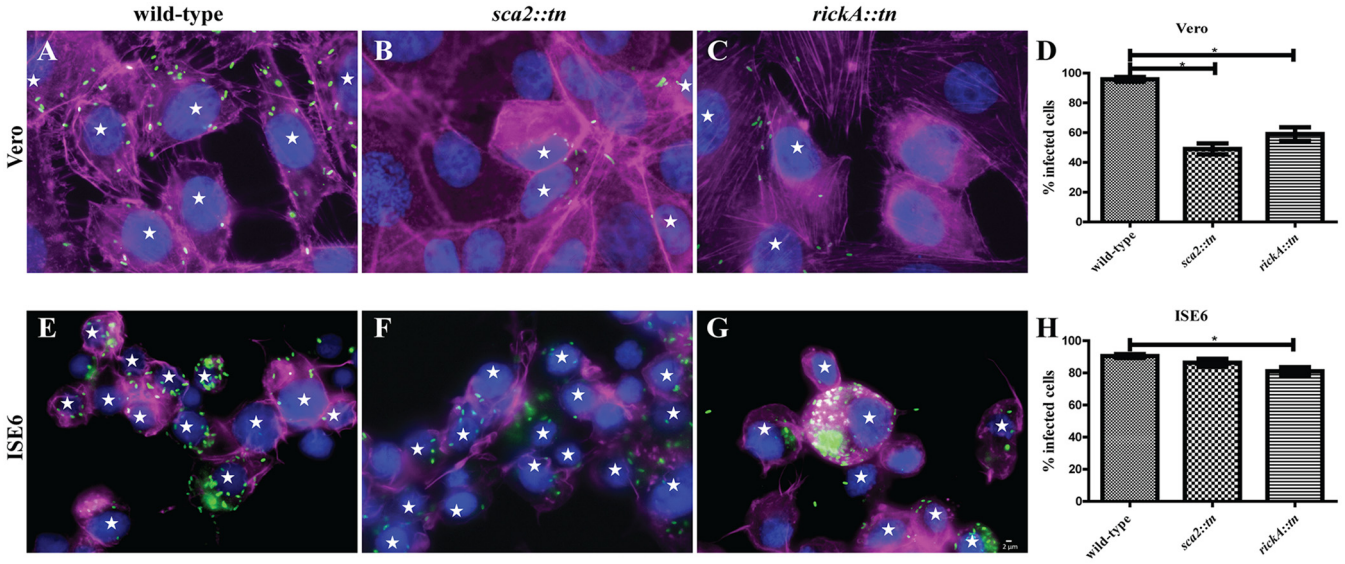

FIG 5 Percentage of *R. parkeri*-infected Vero and ISE6 cells at 24 hpi. Epifluorescence microscopy of Vero (A to C) or ISE6 (E to G) cells infected with *R. parkeri* wild type (A and E), *R. parkeri sca2*::*tn* (B and F), and *R. parkeri rickA*::*tn* (C and G). Cells were stained for *Rickettsia* (green), nuclear material (blue), and actin (magenta). (D and H) Graphical representation of percent infected Vero (D) and ISE6 (H) cells. Data are representative of two replicates per experiment and two independent experiments. Statistical analysis consisted of a one-way ANOVA with Tukey's *post hoc* analysis. $P < 0.05$. White scale bar, 2 μm. Stars indicate cells infected with *Rickettsia*.

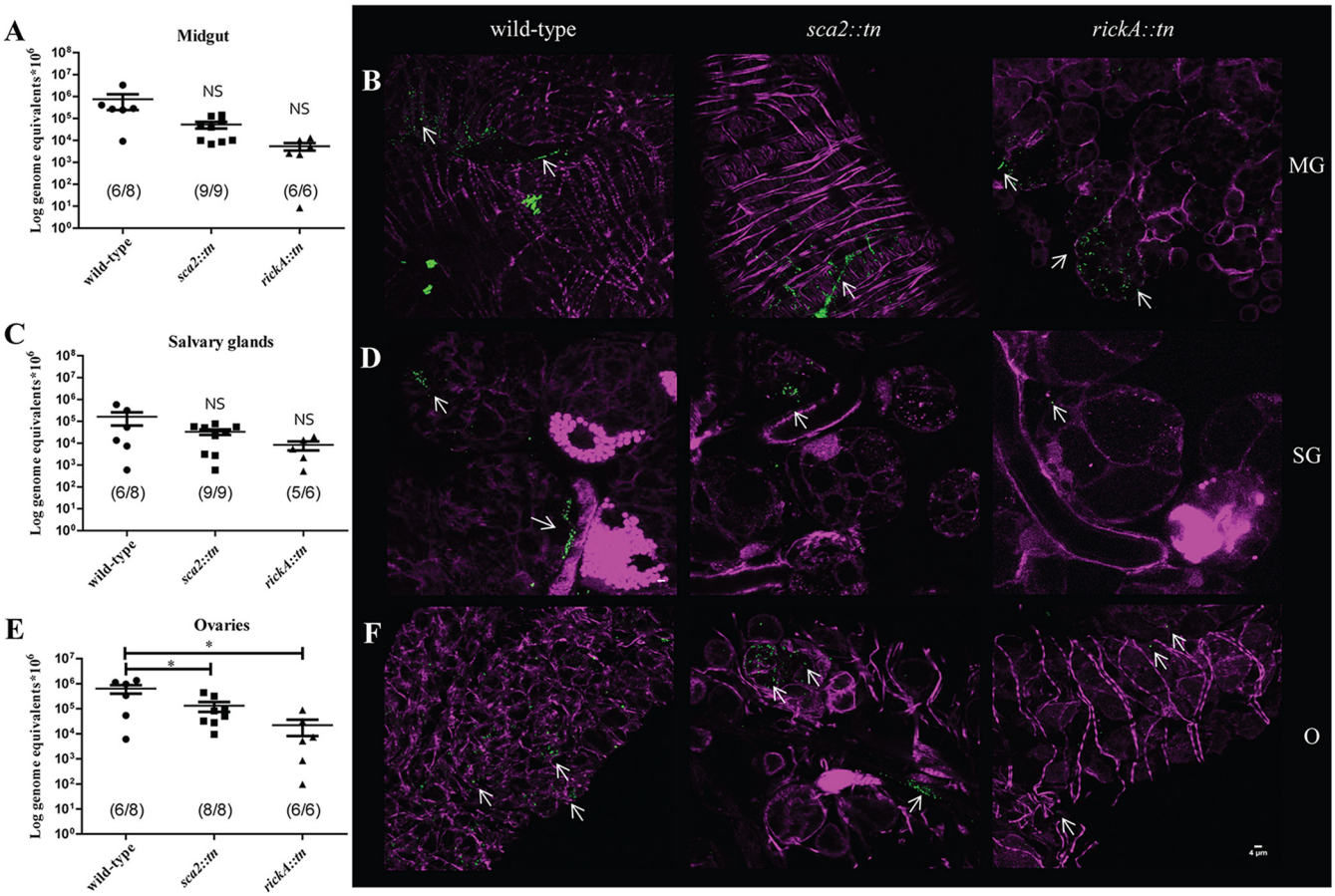

FIG 6 Dissemination of *R. parkeri* wild-type, *sca2*::*tn*, and *rickA*::*tn* in *A. maculatum* at 12 hpe. Mean rickettsial load as quantified by qPCR for the midgut (A), salivary glands (C), and ovaries (E). Inset values represent the number of infected ticks over the number of total ticks tested via qPCR. (B) Confocal microscopy of midgut (B, top), salivary glands (D, middle), and ovaries (F, bottom), corresponding to the data presented in panel A for the *R. parkeri* wild-type (left), *sca2*::*tn* (center), and *rickA*::*tn* (right) strains. All tissues were stained for *Rickettsia* (green) and actin (magenta). Statistical analysis consisted of a one-way ANOVA followed by Tukey's *post hoc* analysis, with a *P* value of <0.05 being considered significant (denoted by an asterisk). Error bars represent the SEM. Means are represented by the bar between the SEM. NS indicates nonsignificant data sets compared to wild-type data. Data and images are representative of 2 independent experiments. White scale bar, 4 μm. Arrows indicate rickettsiae.

Evidence of infection in the hemolymph suggests that, much like initial bacterial numbers in the other tick organs assessed here, rickettsial load was highest at 12 hpe (Fig. 9A). This density decreased approximately 3 logs for ticks infected with wild-type *R. parkeri* by 3 dpe (Fig. 9B). At 7 dpe, mean rickettsial load and total number of ticks with detectable wild-type *R. parkeri* were further decreased (Fig. 9B). Overall, there was a 7 log decrease in rickettsial load in the hemolymph from 12 hpe to 7 dpe for ticks infected with wild-type *R. parkeri*. For *A. maculatum* infected with *R. parkeri rickA*::*tn*, rickettsial infection decreased only by 1 log from 12 hpe to 3 dpe (Fig. 9A and B). At 7 dpe, although rickettsial load did not significantly decrease, only one tick retained infection (Fig. 9C). Similarly, there was an approximately 1 log decrease in rickettsial load in ticks infected with *R. parkeri sca2*::*tn* between 12 hpe and 3 dpe, with 50% (4/8) of the ticks with detectable rickettsiae at the latter time point (Fig. 9A and B). At 7 dpe, only 29% (2/7) of the ticks exposed to the *R. parkeri sca2*::*tn* strain remained infected, with overall rickettsial load decreasing approximately 1.5 logs compared to 12 hpe. The incidence and rickettsial load decreased in tick hemolymph throughout blood feeding after exposure to rickettsiae.

DISCUSSION

As intracellular bacteria, SFG *Rickettsia* require host cells to replicate. The critical initial steps in rickettsial pathogenesis include bacterial recognition of, and attachment

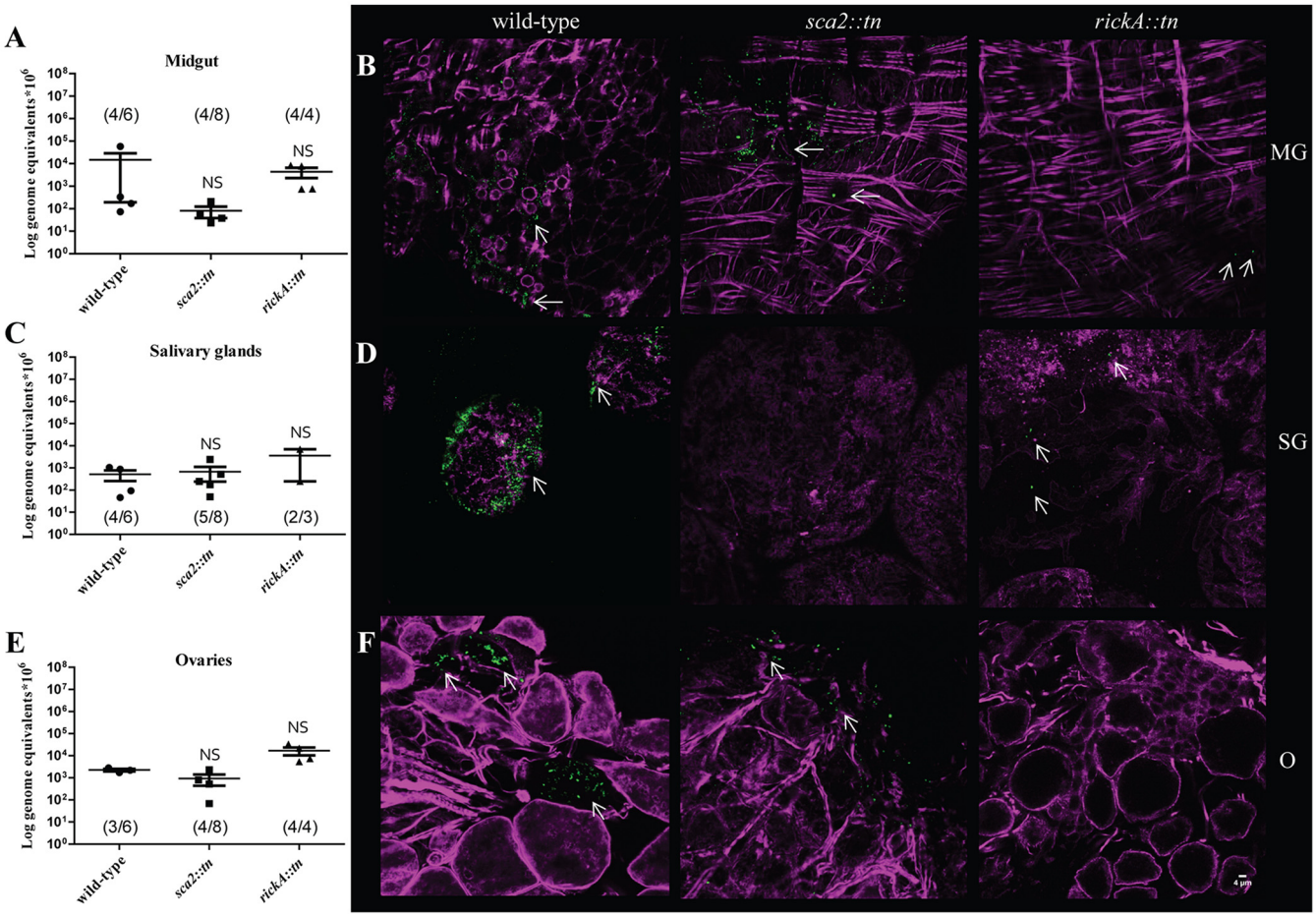

FIG 7 Dissemination of *R. parkeri* wild type, *sca2*::*tn*, and *rickA*::*tn* at 3 dpe. (A, C, and E) Mean rickettsial load as quantified by qPCR for the midgut (A), salivary glands (C), and ovaries (E). Inset values represent the number of infected ticks over the number of total ticks tested via qPCR. (B) Confocal microscopy of midgut (B, top), salivary glands (D, middle), and ovaries (F, bottom), corresponding to the data presented in panel A for *R. parkeri* wild-type (left), *sca2*::*tn* (center), and *rickA*::*tn* (right) strains. All tissues were stained for *Rickettsia* (green) and actin (magenta). Statistical analysis consisted of a one-way ANOVA followed by Tukey's *post hoc* analysis, with a *P* value of <0.05 considered significant (denoted by an asterisk). Error bars represent the SEM. The mean is represented by the bar between the SEM. NS indicates nonsignificant data sets compared to wild-type data. Data and images are representative of 2 independent experiments, excepting the *R. parkeri rickA*::*tn* strain. White scale bar, 4 μm. Arrows indicate rickettsiae.

to, target cells. In vertebrates, SFG *Rickettsia* infect host endothelium, as well as a wide spectrum of phagocytic and nonphagocytic cells (15). Subsequent to invasion of the host cell, rickettsial pathogens undergo ABM to promote cell-to-cell spread during infection *in vitro* (11). Unique to the SFG *Rickettsia* is the presence of two actin-polymerizing proteins. RickA, an activator of the host Arp2/3 complex, was initially proposed to drive motility (8, 16). In addition to being implicated in adherence and invasion, Sca2 was also shown to play a key role in motility, and both motility pathways facilitate cell-to-cell spread in vertebrate cell lines (7, 17). In the current study, a series of experiments was designed to determine if *R. parkeri* Sca2 and RickA display comparable phenotypes in arthropod and mammalian cell lines. *In vitro*, wild-type *R. parkeri* infection in ISE6 cells resulted in larger amounts of initial expression of RickA, which decreased over time. Conversely, expression of Sca2 was low at initial infection time points and increased with time. These observations in tick cells, along with production of actin tails, were consistent with previous studies using only mammalian cells (7). Independent of RickA or Sca2 expression, wild-type and mutant strains shared similar growth kinetics among strains but not between cell lines. In the tick-derived *Ixodes scapularis* cells, replication rates were greater than those in Vero cells. Reasons for the marked difference are not clear but may be due to variations in cell culture conditions,

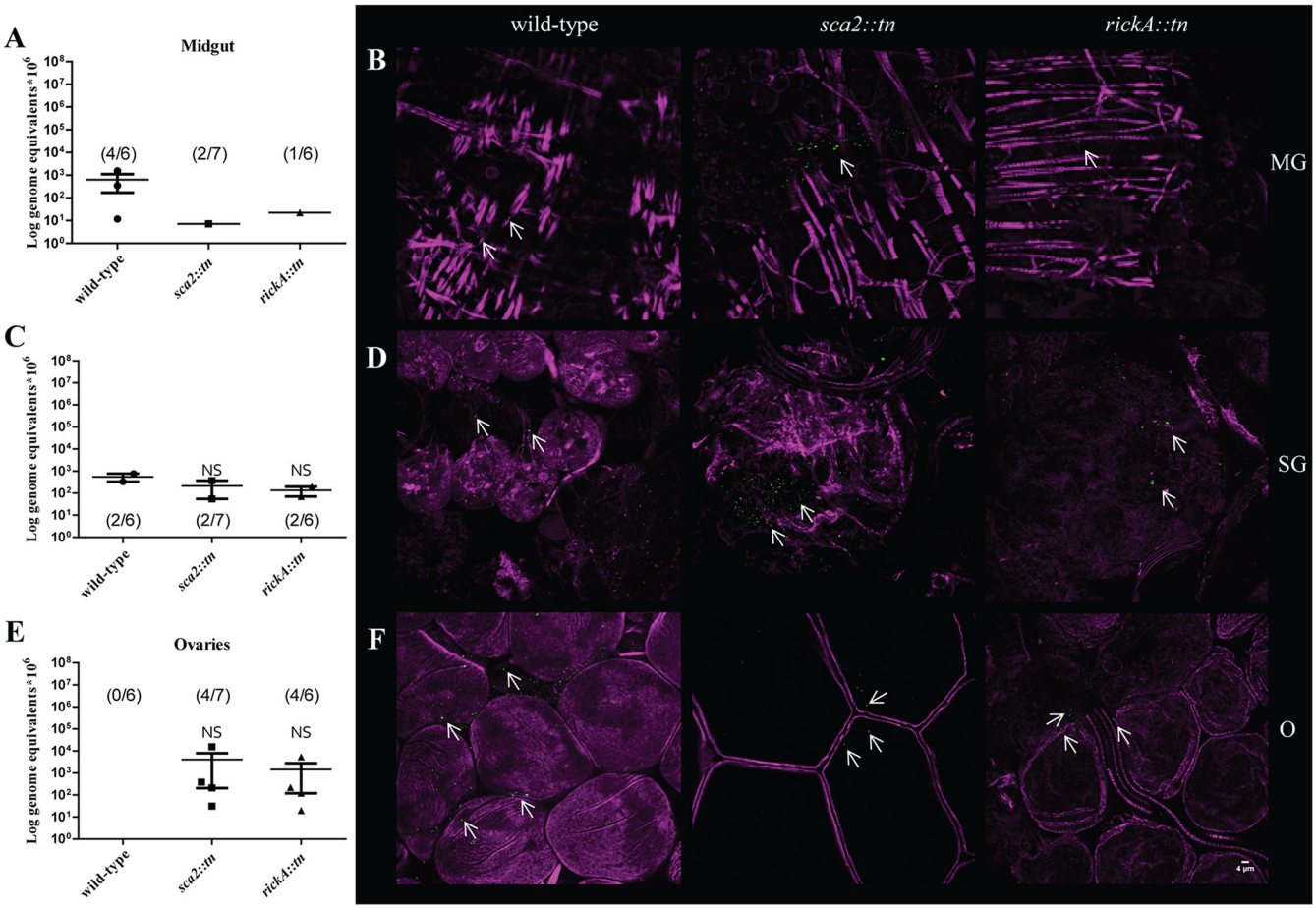

FIG 8 Dissemination of *R. parkeri* wild type, *sca2*::*tn*, and *rickA*::*tn* at 7 dpe. (A, C, and E) Mean rickettsial load as quantified by qPCR for the midgut (A), salivary glands (C), and ovaries (E). Inset values represent the number of infected ticks over the number of total ticks tested via qPCR. (B) Confocal microscopy of midgut (B, top), salivary glands (D, middle), and ovaries (F, bottom), corresponding to the data presented in panel A for *R. parkeri* wild-type (left), *sca2*::*tn* (center), and *rickA*::*tn* (right) strains. All tissues were stained for *Rickettsia* (green) and actin (magenta). Statistical analysis consisted of a one-way ANOVA followed by Tukey's *post hoc* analysis, with a *P* value of <0.05 considered significant (denoted by an asterisk). Error bars represent the SEM. The mean is represented by the bar between the SEM. NS indicates nonsignificant data sets compared to wild-type data. Data and images are representative of 2 independent experiments. White scale bar, 4 μm. Arrows indicate rickettsiae.

which can influence rickettsial growth or the potential for physiological coupling between SFG *Rickettsia* and ticks (18, 19).

Further assessment of actin polymerization by *R. parkeri* strains lacking functional RickA or Sca2 revealed that infection with *R. parkeri rickA*::*tn* resulted in a loss of actin-based polymerization in both ISE6 and Vero cells at 30 mpi; however, actin-based polymerization was observed at 48 hpi. Alternatively, cells infected with *R. parkeri sca2*::*tn* displayed early actin-based polymerization but no late-phase actin polymerization in both ISE6 and Vero cells. Together, the data suggest that *R. parkeri* strains deficient in functional RickA or Sca2 display conserved phenotypes in arthropod and mammalian cells *in vitro*. Observed deficiencies in ABM were expected, as the host protein complexes utilized for actin-based motility, e.g., Arp2/3 complex, are functional in tick cells (20, 21). Interestingly, compared to wild-type *R. parkeri*, decreased late-phase actin polymerization was observed for *R. parkeri rickA*::*tn*, coinciding with reduced cell-to-cell spread. The interaction of specific rickettsial proteins with distinct cell types is not well defined, and while the utility of using rickettsial transformants to examine their interaction with tick cells is promising, it is important to consider that tick-derived cell lines typically originate from embryonic tick cells and often contain multiple, undefined cell types (22, 23). Thus, to expand on the *in vitro* observations, an

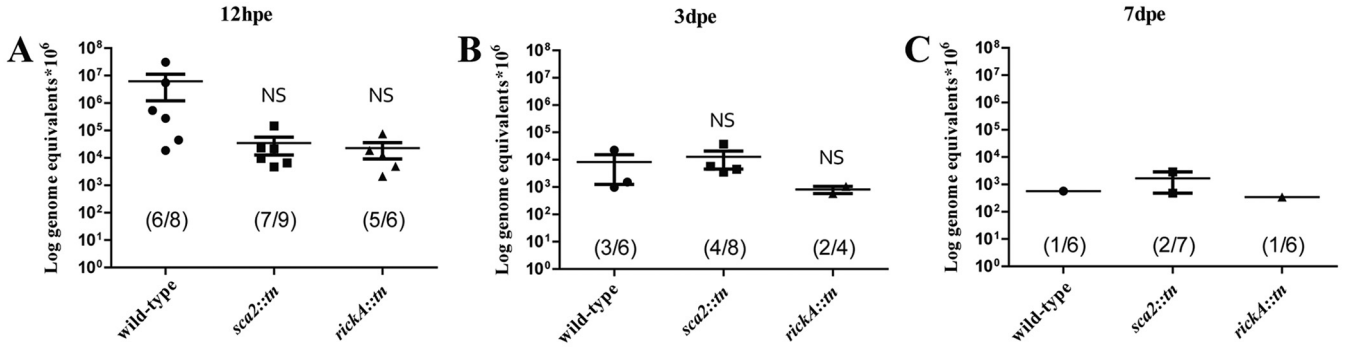

FIG 9 Presence of *R. parkeri* wild type, *sca2*::*tn*, and *rickA*::*tn* in the hemolymph of exposed *A. maculatum*. Mean rickettsial load was quantified at 12 h (left), 3 days (middle), and 7 days (right) postexposure. Statistical analysis consisted of a one-way ANOVA followed by Tukey's *post hoc* analysis, with a *P* value of <0.05 considered significant (denoted by an asterisk). Error bars represent the SEM. The mean is represented by the bar between the SEM. NS indicates nonsignificant data sets compared to wild-type data. Data are representative of two replicates per experiment and two independent experiments.

in vivo infection bioassay was employed in order to determine the contribution of RickA and Sca2 to infection and persistence within the tick host.

The process of infection of ticks by SFG *Rickettsia* has been visualized using genetically modified rickettsiae. The SFG endosymbiont *Rickettsia monacensis* was transformed to express green fluorescent protein (GFP) to observe rickettsial infection in unfixed tick tissues after introduction by capillary feeding (24). While rickettsial survival and dissemination were tick species dependent, GFP-expressing organisms were detected in the gut of ticks up to 4 weeks postexposure (24). In the current study, an established capillary feeding technique (14) was utilized to expose *A. maculatum* to *R. parkeri* wild-type, *rickA*::*tn*, or *sca2*::*tn* strains and produce an infection which was temporally monitored within individual tick tissues. At 12 hpe, *R. parkeri* wild-type, *rickA*::*tn*, and *sca2*::*tn* strains were detected in all organs. Significantly higher levels of wild-type *R. parkeri* than of either mutant strain were present in the ovaries, suggesting that at initial stages of infection RickA and Sca2 are important in rapid dissemination. As the capillary feeding bioassay is beneficial in providing a natural route of exposure (i.e., during bloodmeal acquisition), determining the exact amount of rickettsiae each tick initially receives is not possible and may account for the variation in rickettsial loads in individual organs over time. The nonsignificant variation in rickettsial load in the midgut at 12 hpe suggests that ticks received equivalent amounts of rickettsiae, and the relatively rapid dissemination suggests that the process occurs independently of actual exposure dose. Dissemination to all organs at 12 hpe was a novel observation and highlights the complex nature of rickettsial acquisition by the feeding tick, which consists of multiple organ structures, including the tracheal system, which has previously been hypothesized as a route for producing disseminated infection (24). *Rickettsia*-exposed ticks were allowed to resume bloodmeal acquisition, and at 3 dpe, ticks had comparable levels of rickettsiae present in gut, salivary glands, and ovaries, suggesting the lack of functional RickA or Sca2 did not generate a distinct phenotype. However, at 7 dpe, rickettsial load and the overall percentage of infected ticks were lower than those at 12 hpe and 3 dpe, suggesting that persistent infection waned with prolonged tick feeding. Among the strains, during the exposure period wild-type *R. parkeri* retained the highest infection load in the midgut and the salivary glands but was cleared from the ovaries. Whereas rickettsial loads for both *R. parkeri sca2*::*tn* and *rickA*::*tn* were diminished in all tick organs assessed, they were detectable 1 week postexposure. Thus, these results suggest that the loss of RickA or Sca2 does not negatively impact, and may favor, the persistence phenotype of *R. parkeri* in the tick host.

Both arthropod and rickettsial factors likely contribute to rickettsial dissemination and persistence in the tick host. Upon feeding and rickettsial challenge, upregulation of stress and immune responses are observed in ticks in a tissue-specific manner (25–27). Tick immune molecules may have led to ovarian clearance of wild-type *R. parkeri*, which

displays no defect in motility compared to *R. parkeri sca2*::*tn* and *R. parkeri rickA*::*tn*, suggesting a role for these proteins in tick immune response induction. A similar hypothesis has been proposed for *Rickettsia peacockii*, a species that lacks expression of RickA that was originally thought to confer a persistence phenotype in the ovaries of its tick host, *Dermacentor andersoni* (28). However, genome sequencing has also shown that *R. peacockii* possesses deletions in genes leading to the disruption of *ompA* and *Sca1*, among other genes (29). Thus, the reason *R. peacockii* persists in tick ovaries is unknown at the molecular level, but the ABM-deficient *R. parkeri* mutants utilized in this study support the concept that decreased motility facilitates stable vertical transmission through rickettsial persistence in tick reproductive tissues due to limited exposure to tick immune factors.

Previous data have shown that actin polymerization is the primary mode of rickettsial movement intracellularly (12, 30, 31). The *in vitro* data put forth demonstrate that, like mammalian models, Sca2 and RickA contribute to a pattern of rickettsial ABM in tick cells. However, no implications for ABM by *Rickettsia* in tick hosts could be discerned in the present study. Furthermore, less than 20% of wild-type rickettsiae were observed to polymerize actin at any one time postinfection; thus, it is possible that the microscopy employed failed to accurately capture rickettsial ABM events. Alternatively, it is possible that additional proteins aid in rickettsial dissemination and, therefore, persistence. For instance, Sca4 has recently been identified as a secreted factor that leads to rickettsial protrusion and infection of neighboring cells independent of ABM (32). The role of Sca4 in tick infection and dissemination requires further examination.

In summary, using an appropriate tick host/SFG *Rickettsia* system, the data suggest that while Sca2 and RickA function similarly in arthropod and mammalian cell lines, they are not essential for initial infection and dissemination of *Rickettsia* into tick organs and may influence persistence in tick ovaries. These studies can serve as a model for assessing rickettsial factors that have the potential to contribute to the infection and transmission dynamics of SFG *Rickettsia* within an actively feeding tick host. Furthermore, the roles of Sca2 and RickA, and other suspected SFG *Rickettsia* virulence determinants, such as OmpA (33), as transmission factors can be assessed by examining the interface between ticks and vertebrate hosts.

MATERIALS AND METHODS

Rickettsial strains and purification. *Rickettsia parkeri* wild-type (strain Portsmouth), *R. parkeri sca2*::*tn*, and *R. parkeri rickA*::*tn* strains were derived and propagated as previously published (7, 34, 35). For *in vitro* and *in vivo* bioassays, low-passage-number (≤5) *Rickettsia* organisms were semipurified as previously published (18). Briefly, infected cells were lysed using a 27-gauge needle, followed by centrifugation to separate *Rickettsia* from cell debris, and, finally, supernatant was passed through a 2-μm syringe filter (Whatman). Rickettsial enumeration was performed using a BacLight Live/Dead viability kit (Molecular Probes) with a Petroff-Hausser counting chamber (Hausser Scientific Company) and viewed on a fluorescence microscope (Leica) (36).

***In vitro* infection assays.** Vero cells and *Ixodes scapularis*-derived embryonic (ISE6) cells were cultured as previously described (35, 37). For *in vitro* examination of rickettsial ABM and cell-to-cell spread associated with *R. parkeri* wild-type, *sca2*::*tn*, and *rickA*::*tn* strains via microscopy, cells were seeded onto glass coverslips in 24-well plates. Vero cells were seeded at a density of 5×10^4 cells per well and incubated at 32°C for 24 h prior to infection. Additionally, ISE6 cells were seeded at 2×10^5 cells per well and incubated at 32°C prior to infection. Cells were infected at a multiplicity of infection (MOI) of 50. Contact between the bacteria and host cell was induced by centrifugation at $500 \times g$ for 5 min at room temperature. One hour postinoculation (hpi), medium was replaced to remove unbound bacteria. Coverslips containing infected cells were collected at 30 min postinfection (mpi) and 2, 24, and 48 hpi. All coverslips were rinsed once with phosphate-buffered saline (PBS), followed by immunofluorescence staining.

For growth curve analysis of *R. parkeri* wild type, *sca2*::*tn*, and *rickA*::*tn*, Vero and ISE6 cells were seeded in 96-well plates. Vero cells were seeded at a density of 1×10^3 cells per well and incubated at 34°C prior to experimentation. ISE6 cells were seeded at a density of 5×10^4 cells per well and incubated at 32°C prior to experimentation. All cells were infected with rickettsiae at an MOI of 50 and centrifuged at $500 \times g$ for 5 min at room temperature to induce bacterium-host cell contact. At 1 hpi, medium was replaced to remove unbound bacteria. Cells were collected at 30 mpi and 2, 8, 24, 48, 72, 96, and 120 hpi. Vero cells were dislodged by washing cells once with PBS, incubating with trypsin-EDTA, and adding fresh media to collect cells. ISE6 cells were recovered by dislodging cells with PBS. All infected cell samples were centrifuged at $2{,}100 \times g$ for 10 min at 4°C, the supernatant removed, and pellets stored at −20°C until processed for genomic DNA (gDNA) extraction.

TABLE 1 List of primers and probes used for qPCR

Primer set or probe[a]	Sequence[b] (5′−3′)	Partial gene amplified	Reference or source
RpompB129FJJ	CAAATGTTGCAGTTCCTCTAAATG	*R. parkeri ompB*	38
RpompB224RJJ	AAAACAAACCGTTAAAACTACCG		
RparompB	FAM-TTTG+A+G+C+A+G+CA-IABkFQ		
AmacMIF.18F	CCAGGGCCTTCTCGATGT	*A. maculatum mif*	28
AmacMIF.99R	CCATGCGCAATTGCAAACC		
AmacMIF.63	HEX-TGTTCTCCTTTGGACTCAGGCAGC		
Vero b-actin.61F	TGAAGTGTGACGTGGACATCCATA	Vero *β-actin*	29
Vero b-actin.170 R	GGCAGTAATCTCCTTCTGCATCCT		
Vero b-actin.116	TGGCACCACCATGTACCCTGGCATTGCT		
ISE6_calFW	AGCAGGGAACTTTCAAGCTG	*I. scapularis crt*	This paper
ISE6_calREV	AGAAAGGCTCGAACTTGGTG		
ISE6_cal.67	HEX-AGACCTCTGAAGATGCCCGCTTT		

[a]A plus sign denotes the use of a locked nucleic acid.
[b]FAM, 6-carboxyfluorescein; IABkFQ, Iowa Black dark quencher; HEX, hexachlorofluorescein.

For protein analysis of Sca2 and RickA expression in wild-type *R. parkeri* via immunoblotting, Vero and ISE6 cells were seeded in 6-well plates. Vero cells were seeded at a density of 1×10^5 cells per well and incubated at 34°C prior to experimentation. ISE6 cells were seeded at a density of 5×10^6 cells per well and incubated at 32°C prior to experimentation. All cells were infected with rickettsiae at an MOI of 50 and centrifuged at $500 \times g$ for 5 min at room temperature to induce bacterium-host cell contact. At 1 hpi, medium was replaced to remove unbound bacteria. Cells were collected at 30 mpi and 8 and 48 hpi. Infected cells were collected by replacing media with PBS, lifted with a cell scraper, washed twice in PBS via centrifugation at $2{,}100 \times g$ for 5 min at 4°C, and resuspended in radioimmunoprecipitation assay (RIPA) buffer containing protease inhibitor cocktail (Roche). Samples were sonicated, followed by low-speed centrifugation to remove cell debris, and stored at −80°C prior to SDS-PAGE analysis.

SDS-PAGE and immunoblotting. Equal volumes of protein were mixed with 2× Laemmli sample buffer (Bio-Rad) and boiled at 95°C for 10 min prior to loading onto SDS-PAGE gels (Bio-Rad). Protein was transferred to polyvinylidene difluoride (PVDF) membranes and blocked overnight with 3% bovine serum albumin (BSA) (Sigma) at 4°C. Individual membranes were probed with primary anti-Sca2 or anti-RickA antibody followed by IRDye goat anti-rabbit IgG 800 (LI-COR) secondary antibody (7, 11). Membranes were then probed with mouse β-actin primary antibody (Sigma), followed by IRDye donkey anti-mouse IgG 680 (LI-COR) secondary antibody to assess the protein-loading control. Blotted membranes were visualized using a LI-COR Odyssey CLx. Images were imported into Fiji and analyzed by identifying protein signal values of Sca2 or RickA normalized to respective loading controls.

***Amblyomma maculatum*.** *Rickettsia*-free *A. maculatum* was either maintained at the Louisiana State University School of Veterinary Medicine (LSU-SVM) using methods previously described or provided by the Centers for Disease Control and Prevention for distribution by BEI Resources, NIAID, NIH (adult *A. maculatum*, NR-44382) (38–40). All ticks were maintained in a controlled environmental chamber at 27°C with 92% relative humidity and a 12:12 h (light:dark) cycle prior to experimentation.

***In vivo A. maculatum* dissemination assays via capillary feeding technique.** For dissemination assays, 20 female and 6 to 10 male *A. maculatum* organisms were encapsulated and prefed on guinea pigs for 3 to 4 days. Subsequently, female ticks were forcibly removed with forceps and restrained for the capillary feeding technique (1, 14). Briefly, ticks were made to adhere to a petri dish dorsum side down, and capillary tubes (25 μl) (Kimble-Chase) containing 2 μl of rhodamine B and *Rickettsia*, at a concentration of 5×10^7 rickettsiae/μl, were fitted over the hypostome. Ticks were placed in a humidified incubator set at 37°C for 12 h to allow for acquisition of infectious dose. Postincubation ticks were removed from petri dishes and serially washed in 70% ethanol and deionized water to remove nonimbibed media from the tick surface. Ingestion of Rhodamine B was visualized via a fluorescence dissecting microscope. Nonfluorescently labeled *A. maculatum* was excluded from further study. Positively labeled ticks were separated into three groups: (i) 12 h postexposure (hpe), (ii) 3 days postexposure (dpe), and (iii) 7 dpe. Group i was dissected immediately after capillary feeding. Groups ii and iii were returned to their original host guinea pig and allowed to feed for the designated number of days, at which point they were removed and dissected, and individual midgut, salivary gland, ovaries, and hemolymph tissues were processed for gDNA as previously described (41). A portion of each organ, excluding the hemolymph, was utilized for immunofluorescence assay (IFA) for all ticks and time points. For all tick feeding assays, adult *A. maculatum* organisms were fed on Hartley guinea pigs (Charles River Laboratories) in accordance with the LSU-SVM Institutional Care and Use Committee (IACUC) under approved protocol number 15-115.

gDNA extractions and qPCR. All gDNA was extracted via a Qiagen DNeasy blood and tissue kit (Qiagen) and eluted into 35 μl of RNase/DNase-free water for all *in vitro* and *in vivo* samples. Minor modifications for tick tissue extractions were as follows. Briefly, tick tissues were snap-frozen in liquid nitrogen and ground with a pestle, followed by incubation with proteinase K for 5 h at 56°C. All further steps were carried out according to the manufacturer's protocol. An environmental control extraction was included alongside experimental samples. All samples were evaluated via quantitative real-time PCR (qPCR) on a Roche LightCycler 480II (Roche) using gene-specific primers and probes (Table 1). Amplicons for each primer set were incorporated into pCR4-TOPO, and resultant plasmids were

serially diluted to serve as internal standards for each assay. Standards of known copy number, as well as environmental and negative (water) controls, were included along with experimental samples in each set of reactions. Rickettsial infection density was calculated as a ratio of rickettsial copy number to host cell copy number as determined by the absolute quantitation result of qPCR. For *in vivo* tick organs, the ratio was then extrapolated to represent 10^6 cells, equaling the average *A. maculatum* cell number quantified via qPCR.

Immunofluorescence assay. All incubations with coverslips from *in vitro* assays or tick tissues from *in vivo* bioassays were completed at room temperature in a humidified chamber. *In vitro* and *in vivo* samples were washed once in PBS and fixed with 4% paraformaldehyde with 4% sucrose in PBS for 15 min. Samples were permeabilized with 0.1% Triton X-100 in PBS for 15 min and then blocked with 3% BSA in PBS for 1 h. Antibodies were diluted in 1% BSA (Sigma-Aldrich) in PBS. For detection of rickettsiae, RC_{PFA} was utilized followed by goat anti-rabbit Alexa Fluor 488 (Molecular Probes) (42). Samples were washed 3 times with PBS to remove unbound antibody. DAPI (4′,6-diamidino-2-phenylindole dihydrochloride) was utilized for nuclear staining. Cytoskeletal structure of host cells was visualized using Phalloidin-X-Alexa Fluor 568 (Molecular Probes) for *in vitro* samples or Phalloidin-X-Alexa Fluor 647 (Molecular Probes) for *in vivo* tick tissues. A negative-control (no primary antibody) sample was stained in tandem with experimental samples. All samples were mounted with Mowiol (43), sealed, and stored at 4°C until imaged.

Imaging and analysis. A TCS SPS confocal microscope (Leica) was utilized for analysis of actin polymerization and *Rickettsia* infection *in vivo* and *in vitro*. For analysis of *in vitro* actin polymerization, 10 random images were taken for each treatment group and time point. All images were then imported into Fiji software and adjusted for brightness and contrast, followed by using the smoothing tool (44). Actin tails were enumerated using the cell counter plugin. The cell-to-cell spread of rickettsiae *in vitro* was determined by capturing 10 random images across each treatment group at 24 hpi. Infected and noninfected nuclei were then counted to yield the average percentage of infected cells. Postanalysis, all images were adjusted for brightness, contrast, and smoothness in Fiji software. For Image S3 in the supplemental material, a z-stack consisting of 20 image slices was compiled in Fiji by first importing all stacks with the Bio-Formats Importer and then compiled using the z-project tool. All images were compiled into figures using Adobe Illustrator.

Statistical analysis. Statistical analysis consisted of Kruskal-Wallis test followed by Dunn's test for growth curve analysis, a *t* test for assessment of actin polymerization, and a one-way analysis of variance (ANOVA) with Tukey's *post hoc* test for the cell-to-cell spread assay and all *in vivo* analyses. All statistical analyses were administered using GraphPad Prism software. A P value of <0.05 was considered significant for all experiments. Statistical analysis was completed using non-log-transformed data. For graphical representation, data were presented on a log scale, with error bars representing the means ± standard errors of the means (SEM).

SUPPLEMENTAL MATERIAL

Supplemental material for this article may be found at https://doi.org/10.1128/IAI.00123-18.

SUPPLEMENTAL FILE 1, PDF file, 4.2 MB.
SUPPLEMENTAL FILE 2, PDF file, 5.3 MB.
SUPPLEMENTAL FILE 3, PDF file, 3.5 MB.
SUPPLEMENTAL FILE 4, PDF file, 7.6 MB.
SUPPLEMENTAL FILE 5, DOCX file, 0.1 MB.

ACKNOWLEDGMENTS

We thank Michael Levin (CDC) for providing *Rickettsia*-free *A. maculatum* and Christopher Paddock (CDC) for wild-type *R. parkeri* (strain Portsmouth).

This work was supported by the National Institutes of Health (AI077784 to K.R.M. and AI109044 to M.D.W.).

REFERENCES

1. Harris EK, Verhoeve VI, Banajee KH, Macaluso JA, Azad AF, Macaluso KR. 2017. Comparative vertical transmission of *Rickettsia* by *Dermacentor variabilis* and *Amblyomma maculatum*. Ticks Tick Borne Dis 8:598–604. https://doi.org/10.1016/j.ttbdis.2017.04.003.
2. Paddock CD, Finley RW, Wright CS, Robinson HN, Schrodt BJ, Lane CC, Ekenna O, Blass MA, Tamminga CL, Ohl CA, McLellan SL, Goddard J, Holman RC, Openshaw JJ, Sumner JW, Zaki SR, Eremeeva ME. 2008. *Rickettsia parkeri* rickettsiosis and its clinical distinction from Rocky Mountain spotted fever. Clin Infect Dis 47:1188–1196. https://doi.org/10.1086/592254.
3. Lin L, Decker CF. 2012. Rocky Mountain spotted fever. Dis Mon 58:361–369. https://doi.org/10.1016/j.disamonth.2012.03.008.
4. Drexler NA, Dahlgren FS, Heitman KN, Massung RF, Paddock CD, Behravesh CB. 2016. National surveillance of spotted fever group rickettsioses in the United States, 2008-2012. Am J Trop Med Hyg 94:26–34. https://doi.org/10.4269/ajtmh.15-0472.
5. Paddock CD. 2009. The science and fiction of emerging rickettsioses. Ann N Y Acad Sci 1166:133–143. https://doi.org/10.1111/j.1749-6632.2009.04529.x.
6. Paddock CD, Goddard J. 2015. The evolving medical and veterinary importance of the Gulf Coast tick (Acari: Ixodidae). J Med Entomol 52:230–252. https://doi.org/10.1093/jme/tju022.
7. Reed SC, Lamason RL, Risca VI, Abernathy E, Welch MD. 2014. *Rickettsia* actin-based motility occurs in distinct phases mediated by different actin nucleators. Curr Biol 24:98–103. https://doi.org/10.1016/j.cub.2013.11.025.

8. Gouin E, Egile C, Dehoux P, Villiers V, Adams J, Gertler F, Li R, Cossart P. 2004. The RickA protein of *Rickettsia conorii* activates the Arp2/3 complex. Nature 427:457–461. https://doi.org/10.1038/nature02318.
9. Madasu Y, Suarez C, Kast DJ, Kovar DR, Dominguez R. 2013. *Rickettsia* Sca2 has evolved formin-like activity through a different molecular mechanism. Proc Natl Acad Sci U S A 110:E2677–E2686. https://doi.org/10.1073/pnas.1307235110.
10. Cardwell MM, Martinez JJ. 2012. Identification and characterization of the mammalian association and actin-nucleating domains in the *Rickettsia conorii* autotransporter protein, Sca2. Cell Microbiol 14:1485–1495. https://doi.org/10.1111/j.1462-5822.2012.01815.x.
11. Haglund CM, Choe JE, Skau CT, Kovar DR, Welch MD. 2010. *Rickettsia* Sca2 is a bacterial formin-like mediator of actin-based motility. Nat Cell Biol 12:1057–1063. https://doi.org/10.1038/ncb2109.
12. Heinzen RA, Hayes SF, Peacock MG, Hackstadt T. 1993. Directional actin polymerization associated with spotted fever group *Rickettsia* infection of Vero cells. Infect Immun 61:1926–1935.
13. Simser JA, Rahman MS, Dreher-Lesnick SM, Azad AF. 2005. A novel and naturally occurring transposon, ISRpe1 in the *Rickettsia peacockii* genome disrupting the rickA gene involved in actin-based motility. Mol Microbiol 58:71–79. https://doi.org/10.1111/j.1365-2958.2005.04806.x.
14. Macaluso KR, Sonenshine DE, Ceraul SM, Azad AF. 2001. Infection and transovarial transmission of rickettsiae in *Dermacentor variabilis* ticks acquired by artificial feeding. Vector Borne Zoonotic Dis 1:45–53. https://doi.org/10.1089/153036601750137660.
15. Walker DH. 1997. Endothelial-target rickettsial infection. Lab Anim Sci 47:483–485.
16. Jeng RL, Goley ED, D'Alessio JA, Chaga OY, Svitkina TM, Borisy GG, Heinzen RA, Welch MD. 2004. A *Rickettsia* WASP-like protein activates the Arp2/3 complex and mediates actin-based motility. Cell Microbiol 6:761–769. https://doi.org/10.1111/j.1462-5822.2004.00402.x.
17. Kleba B, Clark TR, Lutter EI, Ellison DW, Hackstadt T. 2010. Disruption of the *Rickettsia rickettsii* Sca2 autotransporter inhibits actin-based motility. Infect Immun 78:2240–2247. https://doi.org/10.1128/IAI.00100-10.
18. Sunyakumthorn P, Bourchookarn A, Pornwiroon W, David C, Barker SA, Macaluso KR. 2008. Characterization and growth of polymorphic *Rickettsia felis* in a tick cell line. Appl Environ Microbiol 74:3151–3158. https://doi.org/10.1128/AEM.00025-08.
19. Munderloh UG, Kurtti TJ. 1995. Cellular and molecular interrelationships between ticks and prokaryotic tick-borne pathogens. Annu Rev Entomol 40:221–243. https://doi.org/10.1146/annurev.en.40.010195.001253.
20. Petchampai N, Sunyakumthorn P, Banajee KH, Verhoeve VI, Kearney MT, Macaluso KR. 2015. Identification of host proteins involved in rickettsial invasion of tick cells. Infect Immun 83:1048–1055. https://doi.org/10.1128/IAI.02888-14.
21. Petchampai N, Sunyakumthorn P, Guillotte ML, Verhoeve VI, Banajee KH, Kearney MT, Macaluso KR. 2014. Novel identification of *Dermacentor variabilis* Arp2/3 complex and its role in rickettsial infection of the arthropod vector. PLoS One 9:e93768. https://doi.org/10.1371/journal.pone.0093768.
22. Kurtti TJ, Munderloh UG, Krueger DE, Johnson RC, Schwan TG. 1993. Adhesion to and invasion of cultured tick (Acarina: Ixodidae) cells by *Borrelia burgdorferi* (Spirochaetales: Spirochaetaceae) and maintenance of infectivity. J Med Entomol 30:586–596. https://doi.org/10.1093/jmedent/30.3.586.
23. Kurtti TJ, Burkhardt NY, Heu CC, Munderloh UG. 2016. Fluorescent protein expressing *Rickettsia buchneri* and *Rickettsia peacockii* for tracking symbiont-tick cell interactions. Vet Sci 3:E34.
24. Baldridge GD, Kurtti TJ, Burkhardt N, Baldridge AS, Nelson CM, Oliva AS, Munderloh UG. 2007. Infection of *Ixodes scapularis* ticks with *Rickettsia monacensis* expressing green fluorescent protein: a model system. J Invertebr Pathol 94:163–174. https://doi.org/10.1016/j.jip.2006.10.003.
25. Macaluso KR, Mulenga A, Simser JA, Azad AF. 2003. Interactions between rickettsiae and *Dermacentor variabilis* ticks: analysis of gene expression. Ann N Y Acad Sci 990:568–572. https://doi.org/10.1111/j.1749-6632.2003.tb07428.x.
26. Mulenga A, Macaluso KR, Simser JA, Azad AF. 2003. Dynamics of *Rickettsia*-tick interactions: identification and characterization of differentially expressed mRNAs in uninfected and infected *Dermacentor variabilis*. Insect Mol Biol 12:185–193. https://doi.org/10.1046/j.1365-2583.2003.00400.x.
27. Sunyakumthorn P, Petchampai N, Grasperge BJ, Kearney MT, Sonenshine DE, Macaluso KR. 2013. Gene expression of tissue-specific molecules in ex vivo *Dermacentor variabilis* (Acari: Ixodidae) during rickettsial exposure. J Med Entomol 50:1089–1096. https://doi.org/10.1603/ME12162.
28. Mattila JT, Munderloh UG, Kurtti TJ. 2007. *Rickettsia peacockii*, an endosymbiont of *Dermacentor andersoni*, does not elicit or inhibit humoral immune responses from immunocompetent *D. andersoni* or *Ixodes scapularis* cell lines. Dev Comp Immunol 31:1095–1106. https://doi.org/10.1016/j.dci.2007.01.011.
29. Felsheim RF, Kurtti TJ, Munderloh UG. 2009. Genome sequence of the endosymbiont *Rickettsia peacockii* and comparison with virulent *Rickettsia rickettsii*: identification of virulence factors. PLoS One 4:e8361. https://doi.org/10.1371/journal.pone.0008361.
30. Welch MD, Reed SC, Haglund CM. 2012. Establishing intracellular infection: escape from the phagosome and intracellular colonization (*Rickettsiaaceae*), p 154–174. *In* Palmer GH, Azad AF (ed), Rickettsiales. ASM Press, Washington, DC.
31. Van Kirk LS, Hayes SF, Heinzen RA. 2000. Ultrastructure of *Rickettsia rickettsii* actin tails and localization of cytoskeletal proteins. Infect Immun 68:4706–4713. https://doi.org/10.1128/IAI.68.8.4706-4713.2000.
32. Lamason RL, Bastounis E, Kafai NM, Serrano R, Del Alamo JC, Theriot JA, Welch MD. 2016. *Rickettsia* Sca4 reduces vinculin-mediated intercellular tension to promote spread. Cell 167:670–683. https://doi.org/10.1016/j.cell.2016.09.023.
33. Noriea NF, Clark TR, Mead D, Hackstadt T. 2017. Proteolytic cleavage of the immunodominant outer membrane protein rOmpA in *Rickettsia rickettsii*. J Bacteriol 199:e00826-16. https://doi.org/10.1128/JB.00826-16.
34. Paddock CD, Sumner JW, Comer JA, Zaki SR, Goldsmith CS, Goddard J, McLellan SL, Tamminga CL, Ohl CA. 2004. *Rickettsia parkeri*: a newly recognized cause of spotted fever rickettsiosis in the United States. Clin Infect Dis 38:805–811. https://doi.org/10.1086/381894.
35. Pornwiroon W, Bourchookarn A, Paddock CD, Macaluso KR. 2009. Proteomic analysis of *Rickettsia parkeri* strain Portsmouth. Infect Immun 77:5262–5271. https://doi.org/10.1128/IAI.00911-09.
36. Kurtti TJ, Simser JA, Baldridge GD, Palmer AT, Munderloh UG. 2005. Factors influencing *in vitro* infectivity and growth of *Rickettsia peacockii* (*Rickettsiales: Rickettsiaceae*), an endosymbiont of the Rocky Mountain wood tick, *Dermacentor andersoni* (Acari, Ixodidae). J Invertebr Pathol 90:177–186. https://doi.org/10.1016/j.jip.2005.09.001.
37. Pornwiroon W, Pourciau SS, Foil LD, Macaluso KR. 2006. *Rickettsia felis* from cat fleas: isolation and culture in a tick-derived cell line. Appl Environ Microbiol 72:5589–5595. https://doi.org/10.1128/AEM.00532-06.
38. Banajee KH, Embers ME, Langohr IM, Doyle LA, Hasenkampf NR, Macaluso KR. 2015. *Amblyomma maculatum* feeding augments *Rickettsia parkeri* infection in a rhesus macaque model: a pilot study. PLoS One 10:e0135175. https://doi.org/10.1371/journal.pone.0135175.
39. Grasperge BJ, Morgan TW, Paddock CD, Peterson KE, Macaluso KR. 2014. Feeding by *Amblyomma maculatum* (Acari: Ixodidae) enhances *Rickettsia parkeri* (Rickettsiales: Rickettsiaceae) infection in the skin. J Med Entomol 51:855–863. https://doi.org/10.1603/ME13248.
40. Troughton DR, Levin ML. 2007. Life cycles of seven ixodid tick species (Acari: Ixodidae) under standardized laboratory conditions. J Med Entomol 44:732–740. https://doi.org/10.1093/jmedent/44.5.732.
41. Sunyakumthorn P, Petchampai N, Kearney MT, Sonenshine DE, Macaluso KR. 2012. Molecular characterization and tissue-specific gene expression of *Dermacentor variabilis* alpha-catenin in response to rickettsial infection. Insect Mol Biol 21:197–204. https://doi.org/10.1111/j.1365-2583.2011.01126.x.
42. Chan YG, Riley SP, Chen E, Martinez JJ. 2011. Molecular basis of immunity to rickettsial infection conferred through outer membrane protein B. Infect Immun 79:2303–2313. https://doi.org/10.1128/IAI.01324-10.
43. Harlow E, Lane D. 2006. Mounting samples in Gelvatol or Mowiol. CSH Protoc 2006:pdb.prot4461.
44. Schindelin J, Arganda-Carreras I, Frise E, Kaynig V, Longair M, Pietzsch T, Preibisch S, Rueden C, Saalfeld S, Schmid B, Tinevez JY, White DJ, Hartenstein V, Eliceiri K, Tomancak P, Cardona A. 2012. Fiji: an open-source platform for biological-image analysis. Nat Methods 9:676–682. https://doi.org/10.1038/nmeth.2019.